Supplemental Material

The BAH domain of Rsc2 is a histone H3 binding domain

Anna L. Chambers, Laurence H. Pearl, Antony W. Oliver, and Jessica A. Downs

Table S1. Mean enrichment of Rsc2-myc proteins by ChIP expressed as % of input. Data for untagged control samples are shown in brackets. ND = not determined.

Locus	Full-length Rsc2	Rsc2-BAH-CT1	BAH-CT1-W436A	BAH-CT1-W436L	BAH-CT1-K437E
25S	2.2 (0.3)	ND	ND	ND	ND
Epro	0.2 (0.05)	ND	ND	ND	ND
CAR	17.9 (0.9)	ND	ND	ND	ND
18S-A	2.6 (0.1)	ND	ND	ND	ND
18S-B	1.1 (0.1)	3.0 (0.6)	2.2 (0.6)	2.4 (0.6)	3.0 (0.6)
HTA1	19.3 (0.3)	15 (1.8)	3.1 (1.8)	1.9 (1.8)	11.56 (1.8)
HTZ1	ND	10 (0.3)	3.2 (0.3)	2.7 (0.3)	6.7 (0.3)

Table S2. Yeast strains used in this study

Strain	Genotype	Reference
DMY2804	W303a *RDN1-NTS1::mURA3*	(1)
DMY2835	*sir2::Kan*^{R} in DMY2804	(2)
JDY790	*rsc2*::KanMX6 in DMY2804	This study
JDY822	*rsc2*::*TRP1* in DMY2835	This study
YNK179-191	*rsc2*::KanMX6 in JKM179 (*MAT*α, *ade1-100*, *leu2-3,112*, *lys5*, *trp1::hisG*, *ura3-52*, *ho*Δ, *hml*Δ, *hmr*Δ,*ade3::GAL1pro::HO*)	(3)
rsc2-BY4741	*rsc2*::KanMX4 in BY4741	Euroscarf deletion collection
YB109	*MAT*α *ura3-52 his3-*Δ*200 ade2-101 trp1-*Δ*1 gal3*$^{-}$*leu2-3, 112 GAL1::his3-*Δ*5' trp1::his3-*Δ*3'::HOcs lys2*$^{-}$ *(leaky)*	(4)
JPY12	MATa *his3-200 leu2-1 lys2-0 trp1-63 ura3-167 met15-0 ade2::hisG RDN1::mURA3/HIS3 RDN1::Ty1-Met15 TELV::ADE2 hht2-hhf2::hygMX hht1 hhf1::natMX pJP11 (LYS2 CEN HHT1-HHF1)*	(5)
JDY826	As JPY12, but with pJP15-A75V (*LEU2 CEN hht1-A75V HHF1*) instead of pJP11	This study (Plasmid was kind gift of J. Boeke and A. Norris)

Table S3. Yeast plasmids used in this study

Plasmid	Name	Description
pRsc2-myc	pJD629	*RSC2* with 13-myc C-terminal tag under the control of its own promoter with *TRP1* marker in pRS416 backbone
pRsc2-W436A-myc	pJD755	As pJD629 but with W436E substitution
pRsc2-W436L-myc	pJD756	As pJD629 but with W436L substitution
pRsc2-K437E-myc	pJD757	As pJD629 but with K437E substitution
p413GPD (EV)	p413GPD	Empty vector - contains GAPDH constitutive promoter (ATCC 87354)
pGPD-BAH-CT1-myc	pJD625	Overexpression plasmid of Rsc2 BAH-CT1 (aa 401-641) with a C-terminal 13-myc tag cloned into p413GPD
p413-ADHmyc (EV)	pJD616	Empty vector – contains ADH constitutive promoter (ATCC 87370), and 13myc repeat (not expressed)
pADH-BAH-CT1-myc	pJD621	Overexpression plasmid with BAH-CT1 (aa 410-641) cloned into pJD616, with C-terminal in-frame myc tag
pADH-BAH-W436A-myc	pJD758	As pJD621 but with W436A substitution
pADH-BAH-W436L-myc	pJD761	As pJD621 but with W436L substitution
pADH-BAH-K437E-myc	pJD760	As pJD621 but with K437E substitution

Yeast plasmid construction

RSC2 coding sequence and DNA 700 bp upstream and 200 bp downstream was amplified from genomic DNA and cloned into pRS416 to generate pJD578. pJD629 was generated by introduction of a C-terminal 13-myc and *TRP1* into pJD578 using the method of (6).

Plasmids pJD755, pJD756 and pJD757 expressing C-terminally 13myc-tagged Rsc2 containing the substitutions W436A, W436L and K437E respectively, were created by site directed mutagenesis.

To create pJD616, 13-myc repeats were amplified by PCR and were cloned into the *Bam*HI site of p413ADH. The BAH-CT1 domain (aa401-641) coding sequence of Rsc2 was amplified by PCR and was cloned into the *Xba*I-*Bgl*II sites of pJD616 to generate pJD621. The BAH-CT1-myc cassette was subcloned from pJD621 into the GAPDH-promoter containing p413GPD to create pJD625. The W436A, W436L and K437E mutations were introduced into pJD621 by site directed mutagenesis to create pJD758, pJD761 and pJD760, respectively.

Recombinant protein expression plasmid construction

For the recombinant His-BAH-CT1 expression plasmid, PCR primers were used to amplify the region encoding the BAH and CT1 domains of *S. cerevisiae* Rsc2 (amino acids 401-641) with additional flanking restriction sites (*Nde*I and *Xho*I) to facilitate cloning into the vector pTWO-E; an in-house modified pET-17b vector (Novagen) engineered to encode a N-terminal, 3C-protease cleavable, His_6 affinity tag.

The GST-tagged Rsc2 BAH-CT1 expression construct for pull-down assays was generated by subcloning from pTWO-E into pTHREE-E using the same restriction enzyme sites; pTHREE-E is an in-house modified pGEX-6P-1 vector (GE Healthcare). Mutations were introduced by site-directed mutagenesis.

To create the GST-$BAH1^{BAF180}$ construct, a synthetic gene construct was purchased from GenScript (Piscataway, USA) corresponding to amino acids 934-1105 of Uniprot Entry Q86U86 (PB1_HUMAN), flanked by *Nde*I and *Eco*RI restriction sites to facilitate sub-cloning into the expression vector pTHREE-E. A construct corresponding to amino acids 361-600 of Uniprot Entry P53236 (RSC1-YEAST) was generated by PCR, using a full-length clone as a template, to create GST-BAH^{Rsc1}. Restriction sites encoded by the PCR primers (*Nde*I/*Xho*I) were used for sub-cloning into the expression vector pTHREE-E.

Expression and purification of His-BAH-CT1

The plasmid encoding His-BAH-CT1 was transformed into the *E.coli* strain Rosetta2 (DE3) pLysS (Merck Chemicals) for expression. 100 ml of L-broth (1% w/v tryptone, 0.5% w/v NaCl, 0.5% w/v yeast extract), supplemented with 100 μg/ml ampicillin and 34 μg/ml chloramphenicol, was inoculated with a single transformed bacterial colony. Following overnight growth at 37 °C, 10 ml was then used to inoculate 1 l of L-broth supplemented, as before, with antibiotics. The culture was grown in at 37 °C and to an A_{600} of ~ 0.6. The temperature was

reduced to 20 ºC and expression of Rsc2-BAH1-CT1 induced by the addition of IPTG to a final concentration of 0.4 mM. The culture was grown for a further 16-18 hours at 20 ºC, after which the cells were harvested by centrifugation (4500 x *g*, 10 minutes, 10 °C), and the pellet stored at -80 °C until required.

The cell pellet arising from 4 l of cell culture was resuspended in 40 ml of buffer A: 50 mM HEPES.NaOH pH 7.5, 250 mM NaCl, 10 mM imidazole. Benzonase nuclease (Merck Chemicals) was added to the suspension (1000 Units), along with a single EDTA-free protease inhibitor tablet (Roche), and the cells disrupted by sonication. Cell debris and insoluble material were then removed by centrifugation at 40,000 x *g* for 30 minutes at 4°C.
The supernatant arising from this step was applied to a batch/gravity column containing 10 ml of Talon affinity resin (TaKaRa Bio) equilibrated in Buffer A. The column containing the cell extract and resin was rotated/rolled at 4 °C for a period of 1 hour to facilitate protein binding. The resin was allowed to pack under gravity, and then washed with successive applications of Buffer A (approximately 250 ml in total). Any retained protein was eluted from the column with the application of Buffer B: 50 mM HEPES.NaOH pH 7.5, 250 mM NaCl, 300 mM imidazole.

Fractions containing Rsc2-BAH-CT1 were identified by SDS-PAGE and then pooled. The affinity tag was cleaved from the protein by the addition of rhinovirus 3C-protease (PreScission protease, GE Healthcare) and incubation overnight at 4 °C.

The cleaved protein was then concentrated to a final volume of 10 ml using Vivaspin 20 (5000 MWCO) centrifugal concentrators (Sartorius Stedim Biotech) before loading onto a HiLoad Superdex 75 size exclusion column (GE Healthcare) equilibrated with Buffer C: 50 mM HEPES.NaOH pH 7.5, 500 mM NaCl, 1 mM TCEP, 1 mM EDTA. Fractions containing BAH-CT1 were again identified by SDS-PAGE, pooled and concentrated as before, to a final concentration of between 14 and 22 mg ml^{-1}, then flash-frozen on dry ice and stored at -80 °C until required.

Expression and purification of GST-BAH fusion proteins

Plasmids expressing GST, or wt or mutant GST-BAH constructs, were transformed into *E.coli* strain Rosetta2 (DE3) pLysS cells as above. 100 ml of Turbo Broth (Athena Enzyme Systems), supplemented with 100 μg/ml ampicillin and 34 μg/ml

chloramphenicol, was inoculated with a single transformed bacterial colony. This was grown at 37 °C until the A_{600} of the cell culture had reached 1, when protein expression was induced by the addition of IPTG to a final concentration of 0.4 mM. The culture was grown for a further 16-18 hours at 20ºC, after which the cells were harvested by centrifugation (4500 x *g*, 10 minutes, 10°C), and the pellet stored at -80°C until required.

The cell pellet arising from 100ml of cell culture was resuspended in 10 ml of buffer A: 50 mM HEPES.NaOH pH 7.5, 1000 mM NaCl, 0.5 mM TCEP, and the cells disrupted by sonication. Cell debris and insoluble material were then removed by centrifugation at 40 000 x *g* for 30 minutes at 4°C. The supernatant arising from this step was applied to a batch/gravity column containing 1 ml of Glutathione Sepharose 4 Fast Flow resin (GE Healthcare) equilibrated in Buffer A. The column containing the cell extract and resin was rotated/rolled at 4°C for a period of 1 hour to facilitate protein binding. The resin was allowed to pack under gravity, and then washed with successive applications of Buffer A (approximately 25 ml in total).

Crystallization trials

Crystallization trials were performed using the vapour-diffusion method in MRC 2 sitting-drop crystallization plates, with 22 mg/ml Rsc2-BAH-CT1, at 20 °C, and by mixing 200 nl of protein with 200 nl of the precipitant solution with diffusion against a well volume of 50 μl. Crystals were obtained in several conditions from commercially available screens (Qiagen).

Crystallization and Data Collection

Conditions were optimized in hanging drop plates at 20°C, mixing 1 µl of protein at 14 mg ml^{-1} with 1 µl of precipitant: 100 mM HEPES.NaOH pH7.5, 0.2M $(NH_4)_2SO_4$, 20-30% w/v PEG 3350, against a well volume of 500 µl — a streak-seeding step was often necessary to produce crystals of a suitable size and quality. Crystals were cryo-protected for data collection by step-wise soaking in buffers containing increasing amounts of glycerol, to a final concentration of 30% (v/v).

Diffraction data were collected to 2.4 Å, on station I02, at the Diamond Light Source, Didcot, UK. Data were integrated and scaled using the software packages iMosflm (7) and Scala/ctruncate from the CCP4 suite (8).

The protein crystallized in spacegroup $P2_1$ with unit-cell dimensions of *a* = 64.09 Å; *b* = 64.07 Å, *c* = 136.84 Å; α,γ = 90 °; β = 95.47°, with 4 molecules comprising the asymmetric unit. Statistics for the data collection are given in Table 1 in main text.

Phasing and Refinement

A solution was determined by molecular replacement using the program PHASER (9) with our previously reported structure of the proximal BAH domain from BAF180 / Polybromo (PDB: 1W4S) as a search model. Iterative cycles of refinement and manual intervention (PHENIX: (10) and Coot: (11)) gave the final model — the quality of which was assessed by using MolProbity (12,13). Details of the model, along with Ramachandran and Molprobity statistics are also given in Table 1 in the main text.

Thermal denaturation profiles of BAH-CT1 proteins

Samples containing 2.5 μM protein and 5 x SYPRO Orange (diluted from a 5000 x stock supplied in DMSO; catalogue number S5692, Sigma-Aldrich) were prepared in 20 mM HEPES.NaOH pH 7.5, 200 mM NaCl, 1 mM TCEP, 1 mM EDTA. Denaturation curves were monitored in 96-well PCR plates in a Roche LightCycler 480 II, using 465 and 580 nm filters for excitation and emission wavelengths, respectively. Temperature midpoints (T_m) for each folded to unfolded transition were determined by non-linear regression fitting of a modified Boltzmann model (14) to normalized data in Prism5 (GraphPad Software)

$$Y = (a_n X + b_n) + \frac{(a_d X + b_d) - (a_n X + b_n)}{1 + e^{\frac{T_m - X}{m}}}$$

where: a_n and a_d are the slopes, b_n and b_d the y-intercepts, of the native and denatured baselines respectively. T_m is the melting temperature, and m a slope factor.

SUPPLEMENTAL REFERENCES

1. Huang, J., Brito, I.L., Villen, J., Gygi, S.P., Amon, A. and Moazed, D. (2006) Inhibition of homologous recombination by a cohesin-associated clamp complex recruited to the rDNA recombination enhancer. *Genes Dev*, **20**, 2887-2901.

2. Tanny, J.C., Kirkpatrick, D.S., Gerber, S.A., Gygi, S.P. and Moazed, D. (2004) Budding yeast silencing complexes and regulation of Sir2 activity by protein-protein interactions. *Mol Cell Biol*, **24**, 6931-6946.
3. Kent, N.A., Chambers, A.L. and Downs, J.A. (2007) Dual Chromatin Remodeling Roles for RSC during DNA Double Strand Break Induction and Repair at the Yeast MAT Locus. *J Biol Chem*, **282**, 27693-27701.
4. DeMase, D., Zeng, L., Cera, C. and Fasullo, M. (2005) The Saccharomyces cerevisiae PDS1 and RAD9 checkpoint genes control different DNA double-strand break repair pathways. *DNA Repair (Amst)*, **4**, 59-69.
5. Norris, A., Bianchet, M.A. and Boeke, J.D. (2008) Compensatory interactions between Sir3p and the nucleosomal LRS surface imply their direct interaction. *PLoS Genet*, **4**, e1000301.
6. Longtine, M.S., McKenzie, A., Demarini, D.J., Shah, N.G., Wach, A., Brachat, A., Philippsen, P. and Pringle, J.R. (1998) Additional modules for versatile and economical PCR-based gene deletion and modification in *Saccharomyces cerevisiae*. *Yeast*, **14**, 953-961.
7. Leslie, A.G.W. (1992) Recent changes to the MOSFLM package for processing film and image plate data. *Joint CCP4 + ESF-EAMCB Newsletter on Protein Crystallography*, **26**.
8. CCP4. (1994) The CCP4 suite: programs for protein crystallography. *Acta Crystallogr D Biol Crystallogr*, **50**, 760-763.
9. McCoy, A.J. (2007) Solving structures of protein complexes by molecular replacement with Phaser. *Acta Crystallogr D Biol Crystallogr*, **63**, 32-41.
10. Adams, P.D., Grosse-Kunstleve, R.W., Hung, L.W., Ioerger, T.R., McCoy, A.J., Moriarty, N.W., Read, R.J., Sacchettini, J.C., Sauter, N.K. and Terwilliger, T.C. (2002) PHENIX: building new software for automated crystallographic structure determination. *Acta Crystallogr D Biol Crystallogr*, **58**, 1948-1954.
11. Emsley, P., Lohkamp, B., Scott, W.G. and Cowtan, K. (2010) Features and Development of Coot. *Acta Crystallogr D Biol Crystallogr*, **66**, 486-501.
12. Chen, V.B., Arendall, W.B., Headd, J.J., Keedy, D.A., Immormino, R.M., Kapral, G.J., Murray, L.W., Richardson, J.S. and Richardson, D.C. (2010) MolProbity: all-atom structure validation for macromolecular crystallography. *Acta Crystallogr D*, **66**, 12-21.
13. Davis, I.W., Murray, L.W., Richardson, J.S. and Richardson, D.C. (2004) MolProbity: structure validation and all-atom contact analysis for nucleic acids and their complexes. *Nucleic Acids Res*, **32**, W615-W619.
14. Ericsson, U.B., Hallberg, B.M., Detitta, G.T., Dekker, N. and Nordlund, P. (2006) Thermofluor-based high-throughput stability optimization of proteins for structural studies. *Analytical biochemistry*, **357**, 289-298.
15. Corpet, F. (1988) Multiple sequence alignment with hierarchical clustering. *Nucleic Acids Res*, **16**, 10881-10890.
16. Livingstone, C.D. and Barton, G.J. (1993) Protein sequence alignments: a strategy for the hierarchical analysis of residue conservation. *Comput Appl Biosci*, **9**, 745-756.
17. Kabsch, W. and Sander, C. (1983) Dictionary of protein secondary structure: pattern recognition of hydrogen-bonded and geometrical features. *Biopolymers*, **22**, 2577-2637.

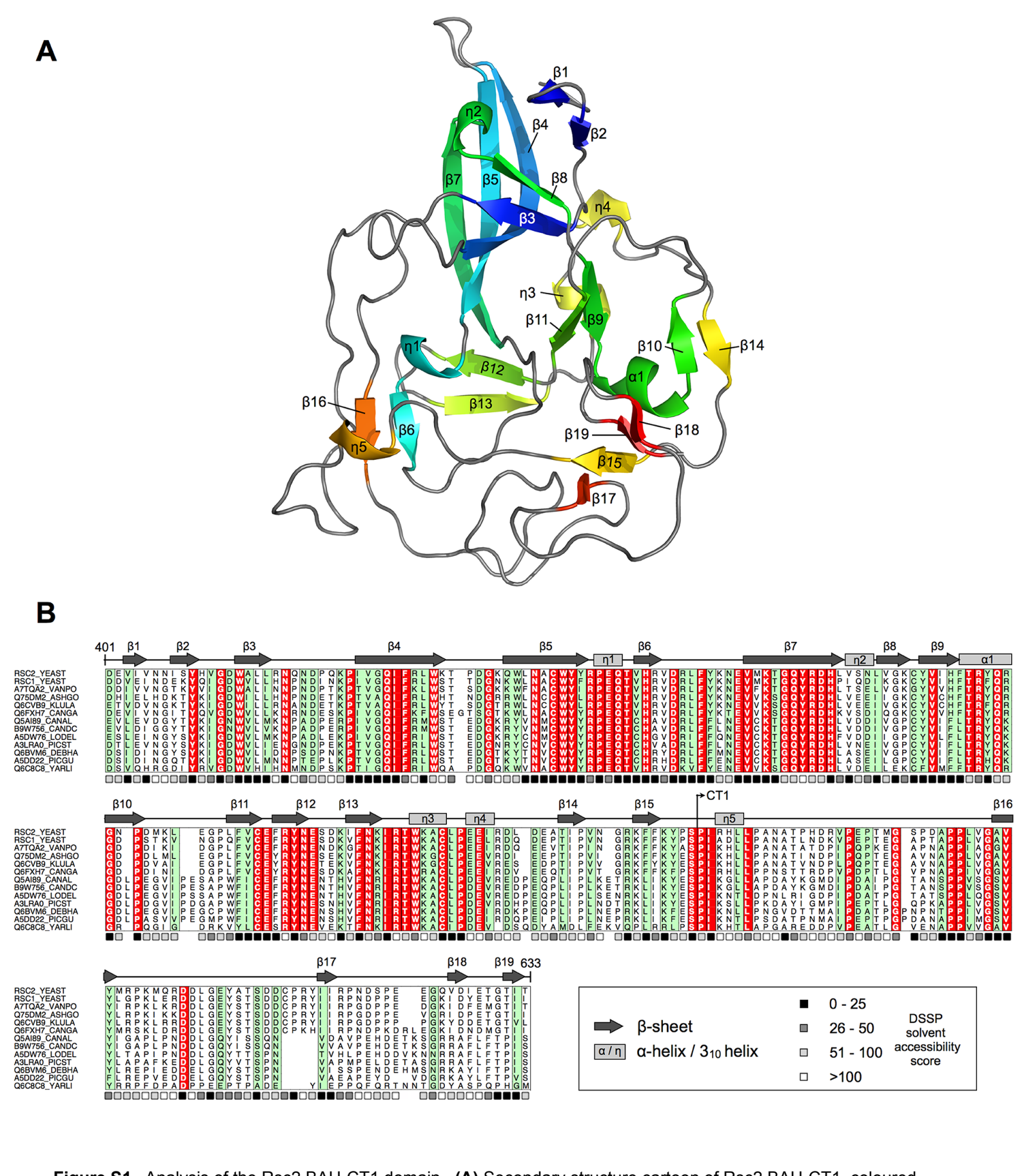

Figure S1. Analysis of the Rsc2 BAH-CT1 domain. **(A)** Secondary structure cartoon of Rsc2 BAH-CT1, coloured from blue through to red, from the visible N-terminus at residue 401 to the C-terminus at residue 633. Secondary structure elements are numbered sequentially from N- to C-terminus. **(B)** Amino acid sequences corresponding to the BAH-CT1 region of Rsc2-related proteins were retrieved from the Uniprot database (using the indicated accession codes), aligned using multi-align (15), then prepared for presentation using AMAS (16). Secondary structure elements corresponding to the Rsc2 BAH-CT1 structure presented in this study are also shown. Solvent accessibility was calculated with DSSP (17) for each amino acid residue of Rsc2 BAH-CT1.

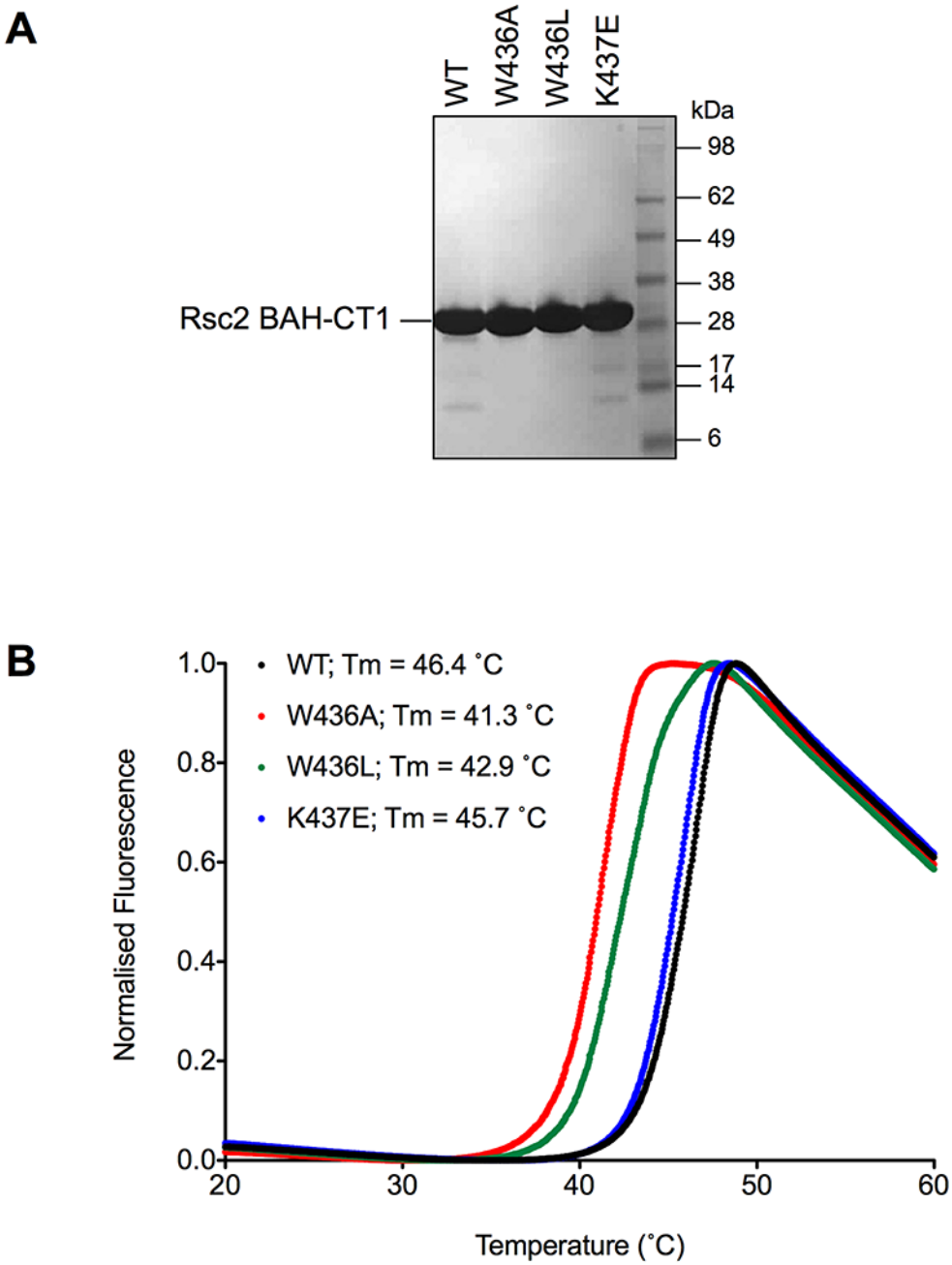

Figure S2 Thermal stability of wild-type and mutant Rsc2 BAH-CT1 proteins. **(A)** SDS-PAGE analysis of purified recombinant Rsc2 BAH-CT1 proteins used for thermal denaturation experiments. **(B)** Thermal denaturation profiles of wt and mutant Rsc2 BAH-CT1 proteins.

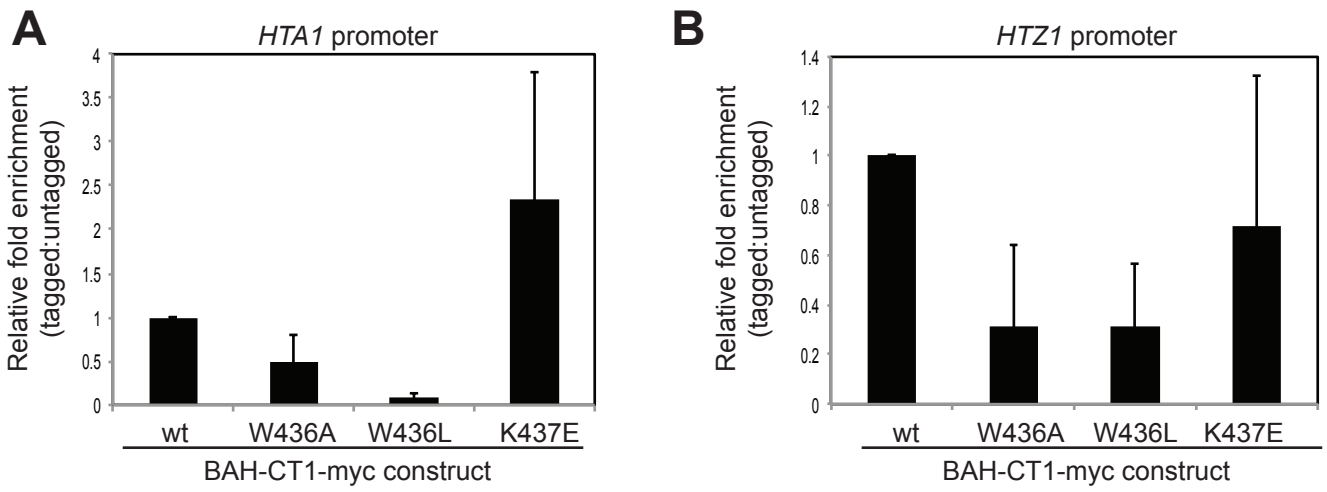

Figure S3 Chromatin association of wild type and mutant Rsc2 BAH-CT1 proteins *in vivo*. **(A and B)** Chromatin immunoprecipitation assays examining enrichment of Myc-tagged overexpressed BAH-CT1 relative to the untagged control at the H2A promoter **(A)** or H2A.Z promoter **(B)**. Data shown are the mean enrichment of at least 3 independent experiments +/- 1 SD. Average % input from the tagged strain (or untagged control strain) is listed in Table S1.